The Company of
Biologists

RESEARCH ARTICLE

Adhesive latching and legless leaping in small, worm-like insect larvae

G. M. Farley[1], M. J. Wise[2], J. S. Harrison[1], G. P. Sutton[3], C. Kuo[4] and S. N. Patek[1,*]

ABSTRACT

Jumping is often achieved using propulsive legs, yet legless leaping has evolved multiple times. We examined the kinematics, energetics and morphology of long-distance jumps produced by the legless larvae of gall midges (*Asphondylia* sp.). They store elastic energy by forming their body into a loop and pressurizing part of their body to form a transient 'leg'. They prevent movement during elastic loading by placing two regions covered with microstructures against each other, which likely serve as a newly described adhesive latch. Once the latch releases, the transient 'leg' launches the body into the air. Their average takeoff speeds (mean: 0.85 m s^{-1}; range: 0.39–1.27 m s^{-1}) and horizontal travel distances (up to 36 times body length or 121 mm) rival those of legged insect jumpers and their mass-specific power density (mean: 910 W kg^{-1}; range: 150–2420 W kg^{-1}) indicates the use of elastic energy storage to launch the jump. Based on the forces reported for other microscale adhesive structures, the adhesive latching surfaces are sufficient to oppose the loading forces prior to jumping. Energetic comparisons of insect larval crawling versus jumping indicate that these jumps are orders of magnitude more efficient than would be possible if the animals had crawled an equivalent distance. These discoveries integrate three vibrant areas in engineering and biology – soft robotics, small, high-acceleration systems, and adhesive systems – and point toward a rich, and as-yet untapped area of biological diversity of worm-like, small, legless jumpers.

KEY WORDS: Latch, Adhesion, Power amplification, Locomotion, Hydrostatic, Elastic

INTRODUCTION

Jumping and hopping are most often achieved with legs – either through the lever-based launches of elongate legs (Astley and Roberts, 2014; Alexander and Vernon, 1975; Zajac et al., 1981; Moore et al., 2017) or through elastically powered short legs (Burrows et al., 2008; Burrows and Sutton, 2008; Bennet-Clark, 1975; Bennet-Clark and Lucey, 1967; Henry et al., 2005; Aerts, 1998). Nevertheless, jumping mechanisms that do not involve legs have evolved in a variety of animals, such as the body-segment torque of click beetles (Evans, 1972, 1973; Ribak and Weihs, 2011), hydrostatic pressurization of a tail-like appendage in springtails

(Brackenbury and Hunt, 1993), and terrestrial tail flips in bony fishes (Ashley-Ross et al., 2014). A particularly intriguing jumping strategy is employed by some small, worm-like animals that use latching, hydrostatic manipulation and elastic mechanisms to launch themselves into the air. This strategy is employed by larvae of certain groups of dipterans (Camazine, 1986; Suenaga et al., 1992; Maitland, 1992; Bonduriansky, 2002; Marinov et al., 2015; Manier and Deamer, 2014) and by nematodes (Campbell and Kaya, 1999a,b). Analogous legless-jumping systems have been discovered several times, yet a basic framework for the biomechanics of worm-like jumpers is needed in order to establish general design principles and interpret the diversity and ecology of these systems.

Legless jumpers can achieve impressive jump performance that rivals that of small, legged jumpers. The jumping flea, a famous small, legged jumper, can jump with speeds of 1.3 m s^{-1} (Sutton and Burrows, 2011), and leafhoppers can accomplish speeds of 1.1 to 2.5 m s^{-1} (Burrows and Sutton, 2008), metrics similar to the 1.98 m s^{-1} takeoff speed of legless fruit fly larvae (*Ceratitis capitata*; Maitland, 1992). Likewise, the click beetle, a hard-bodied legless jumper, can achieve takeoff speeds of 2.4 m s^{-1} (Evans, 1973). Soft-bodied legless jumpers, such as larvae of the piophilid fly *Prochyliza xanthostoma*, have been reported to jump distances 28 times their body length; assuming a takeoff angle of 45 deg, this suggests takeoff speeds of approximately 1 m s^{-1} (Bonduriansky, 2002). Even with the documentation of these intriguing legless systems, most analyses have been limited by imaging technology such that the kinematic capabilities of these systems are uncertain; the fastest recorded frame rate, to our knowledge, of jumping soft-bodied, legless organisms is 54 frames s^{-1} (Camazine, 1986). Recent studies of the hard-bodied click beetle system offered a significant improvement in modeling and energetic calculations through improvements in imaging (Ribak and Weihs, 2011; Ribak et al., 2012).

Small-legged jumping and legless-jumping systems are often powered by elastic mechanisms, typically through latching, elastic loading and release (Longo et al., 2019; Ilton et al., 2018; Sakes et al., 2016; Gronenberg, 1996; Patek, 2015; Patek et al., 2011). Worm-like, legless jumpers typically form a loop with their body by latching their anterior and posterior in place and then springing into the air when the latch is released (Fig. 1). Elastic energy is stored by stretching body surfaces and pressurizing body fluids, much like 'a bent, sausage-shaped balloon' (p. 160, Maitland, 1992). In a study of fruit fly larvae (*Ceratitis capitata*), Maitland (1992) determined that the stored elastic strain energy (31 J kg^{-1}) of the exoskeleton, when experimentally pressurized to 82 mmHg and a strain of 29%, provides just enough energy to launch a jump.

Latching mechanisms are diverse in small, legless systems. For example, gall midge larvae (*Tricholaba barnes*) wedge either the head or anal segments between ventral segments and then load the body into a taut loop (Milne, 1961). Piophilid flies and several species of fruit flies (Tephritidae) reportedly place their mouthparts into the integument on the posterior–ventral side of their body and

[1]Biology Department, Duke University, Durham, NC 27708, USA. [2]Department of Biology, Roanoke College, Salem, VA 24153, USA. [3]School of Life Sciences, University of Lincoln, Lincoln LN6 7TS, UK. [4]Division of Evolutionary Biology, Ludwig Maximilian University of Munich, Grosshaderner Strasse 2, 82152 Planegg-Martinsried, Germany.

*Author for correspondence (snp2@duke.edu)

G.M.F., 0000-0001-5361-7299; M.J.W., 0000-0003-0091-303X; J.S.H., 0000-0001-7752-6471; G.P.S., 0000-0002-3099-9842; C.K., 0000-0002-8533-9358; S.N.P., 0000-0001-9738-882X

Journal of Experimental Biology

1
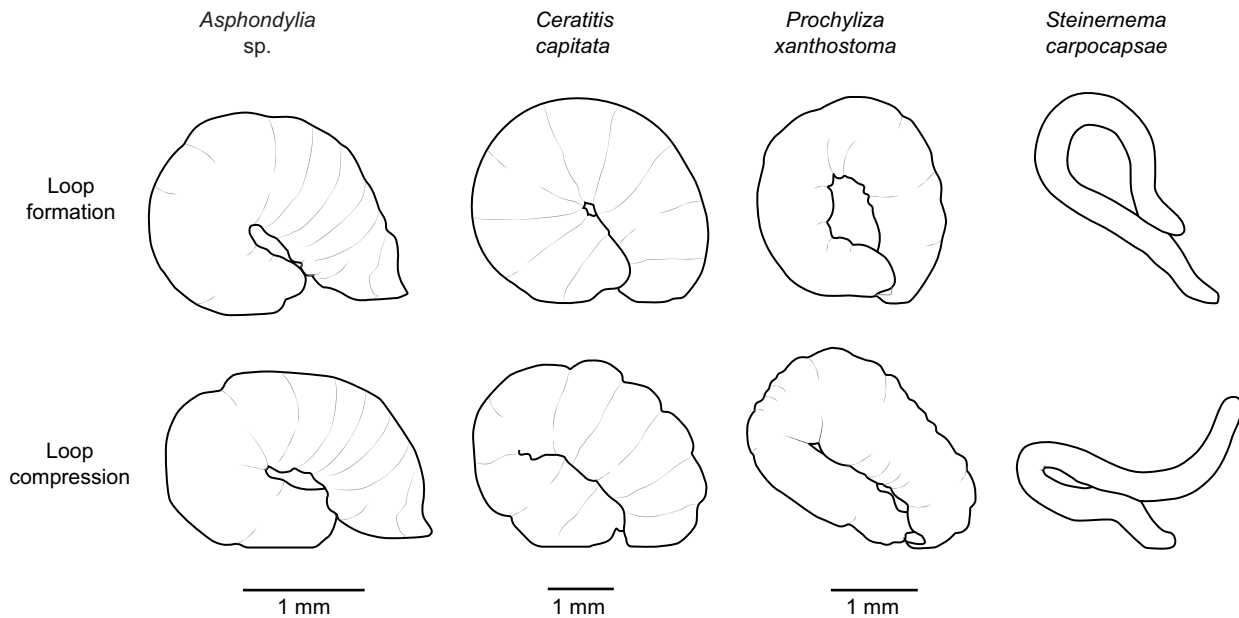
Fig. 1. Many species of soft-bodied, legless larval jumpers form a loop held together by a variety of latch mechanisms and they compress their body prior to jumping. *Asphondylia* sp. larvae exhibit a stereotyped sequence of curling, latching and compressing their body prior to jumping which is similar to the behavior of other soft-bodied legless jumpers reported in the literature. Line drawings were traced from illustrations or photographs from the current study, Maitland (1992), Bonduriansky (2002) and Campbell and Kaya (1999a,b). Segment lines in the illustrations of *Asphondylia* sp. and *Prochyliza xanthostoma* could not clearly be seen in the images, and thus are artistic renderings. Average nematode length was reported as 0.5 mm, but a scale bar for this image was not provided in Campbell & Kaya (1999a,b).

elastically load their body in a loop (Bonduriansky, 2002; Marinov et al., 2015; Maitland, 1992). In addition, Camazine (1986) suggested that fungus gnat larvae (*Mycetophila cingulum*) latch the head and tail together using protolegs or 'pegs'. Finally, microscopic entomopathogenic nematodes (*Steinernema carpocapsae*) use surface tension of water coating the body to adhere the head and tail to form a body loop before jumping (Campbell and Kaya, 1999a, b; Reed and Wallace, 1965). Despite the diversity of legless-jumping mechanisms that have been observed, surprisingly little is known about the morphology and mechanics of the latches that are central to successful jumping.

To elucidate the jumping mechanisms of small, worm-like animals, we studied larvae of an undescribed species of gall midge (*Asphondylia* sp.) that jump when removed from the galls they form on goldenrod plants. We employed high-speed imaging, scanning electron microscopy and mathematical analyses to address the following goals: (1) analyze jump preparation, launch and takeoff dynamics, horizontal travel distance and jump energetics; and (2) establish the morphology and mechanics of latching. We place these specific findings in the broader context of a nascent and phylogenetically diverse field of small, hydrostatic jumpers.

## MATERIALS AND METHODS
Study organisms
Larvae of *Asphondylia* sp. (Diptera: Cecidomyiidae) (Fig. 2A) induce multi-chambered rosette galls in the stem apices of several species of goldenrods (*Solidago*, Asteraceae) (Fig. 2B) (Dorchin et al., 2015). Usually, one larva (but up to three larvae) develop within each chamber, where they develop through three larval instars and pupation, emerging from the galls as adults in early autumn. Mature, third-instar larvae are bright orange, with a fully developed spatula. The spatula is a small, anterior structure near the mouth which, in other species, is used for digging. Second-instar larvae are not only smaller but also generally pale yellow in color

and they do not have a spatula. Only the fully grown third-instar larvae are able to jump when removed from their galls.

Cuttings of *S. bicolor* plants containing *Asphondylia* sp. larvae were collected in Bedford County, VA, USA, in mid-August. In the lab, we extracted larvae from their galls by first peeling away the stiff leaves making up the rosette that surrounded the gall chambers. A hole was then poked into the top of an exposed chamber, whereupon the gall midge larva inside (if healthy) would immediately squeeze its way out. The larvae were quickly placed on a damp paper towel in a covered plastic Petri dish to keep them hydrated until testing. Healthy full-grown third-instar larvae would begin jumping immediately after their exit from a gall.

Jump preparation, launch dynamics and horizontal travel distance
Jump preparation (100 frames s^{-1}) and launch (20,000 frames s^{-1}) were visualized using high-speed imaging (1024×672 pixel
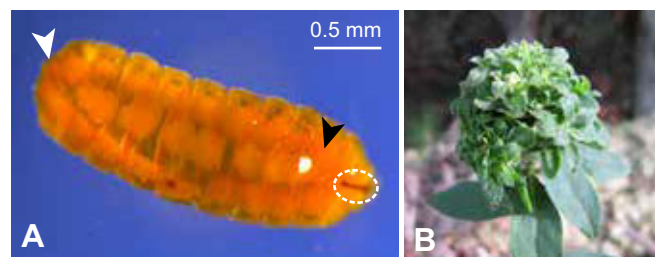
Fig. 2. Larvae of *Asphondylia* sp. develop within galls on silverrod plants. (A) Light microscope image of a third-instar *Asphondylia* sp. larva. Ventral view, anterior is to the right. The posterior-most section of the midge (white arrowhead) and the third segment (black arrowhead) interact to form a latch during the loop formation stage (Fig. 3A). The sternal spatula is indicated with a white dashed ellipse. (B) *Asphondylia* sp. larvae and pupae develop within galls on certain species of goldenrods, such as *Solidago bicolor*.

resolution; Fastcam SA-X2, Photron, San Diego, CA, USA). Each larva was placed on a plastic platform that was illuminated for high-speed imaging (75 W LED, Varsa, Nila, Inc., Altadena, CA, USA). We moved the platform to keep the larva in the camera's focal plane with its lateral side facing the camera. When the larva prepared to jump, we stopped moving the platform and filmed from that position.

Two phases of jump preparation were measured: loop formation (Fig. 3A) and loop contraction (Fig. 3B) (phases are defined in Results). Because of the long duration of jump preparation, we down-sampled the original videos filmed at 20,000 frames s^{-1} to 100 frames s^{-1}, and report these durations with a temporal resolution of 10 ms.

Launch kinematics were autotracked and calculated from high-speed images sampled at the full 20,000 frames s^{-1}. Each image in a video sequence was thresholded to generate a binary image. The thresholded image sequence was then auto-tracked by calculating the center of the body (centroid function, default B&W threshold settings, ImageJ v.1.52a, National Institutes of Health, Bethesda, MD, USA). Tracking began when the larva was in a motionless, curled, pressurized loop position and ended when the larva either was out of focus or left the field of view (Fig. 3C,D). Because most jumps exceeded the field of view, only the initial ascent was tracked in most analyses. For one video sequence, we repeated the auto-tracking process 10 times to calculate digitizing error. Auto-tracking generated a standard error of the mean that constituted 1% of the reported distance and duration measurements.

We measured launch and takeoff kinematics during two distinct time periods. We defined launch as the time period when the body is accelerated before leaving the ground. Therefore, launch began at the first video frame of body movement (latch release) and ended at the first video frame when the body was off the ground (Fig. 3C). Each video was coded by the investigator for the first frame at which

the latch released and the first frame during which the body left the ground. We measured the total duration (t) and distance (d) traveled by the centroid during launch. From this, we calculated average launch power ($P=md^2t^{-3}$) where m is the mass of the whole animal. For mass-specific power output [$P(0.3m)^{-1}$], we conservatively assumed that the larva used one-third of its body mass to launch the system, based on the proportion of the body used for launching (Fig. 3).

We then measured a second time period, which we term takeoff. Takeoff is defined as the time period beginning when the body leaves the ground. We measured the distance traveled by the centroid between each frame before and after the animal leaves the ground. We termed the resulting calculations takeoff speed ($v=dt^{-1}$) and takeoff kinetic energy (KE=$0.5v^2$). In addition, we calculated the angle of takeoff based on the starting and ending position of the centroid relative to the horizontal ground at the start and end of a 1 ms time period after the frame at which the animal leaves the ground.

For each image sequence, body length was measured along the body's midline, and diameter was measured across the body's center (ImageJ v.1.51n). Measurements were calibrated using videos of a millimeter-scale ruler filmed in the plane of focus. The ruler was re-calibrated to 0.1 mm using a 0.02 mm scale under a microscope [KR-814 (1×3) stage micrometer, Klarmann Rulings, Inc., Litchfield, NH, USA]. We weighed the larvae immediately after jumping data were collected (resolution: 0.1 µg; XPE56, Mettler Toledo, Pleasant Prairie, WI, USA).

We performed error (uncertainty) propagation analyses for the launch calculations based on the uncertainty of the mass (balance: 1×10^{-10} kg), distance (calibrated ruler: 2×10^{-5} m) and time measurements (20,000 frames s^{-1} imaging: 5×10^{-5} s). The resulting uncertainty in the reported launch calculations ranged from 10% to 21% (speed: 10%; acceleration: 12%; kinetic energy:
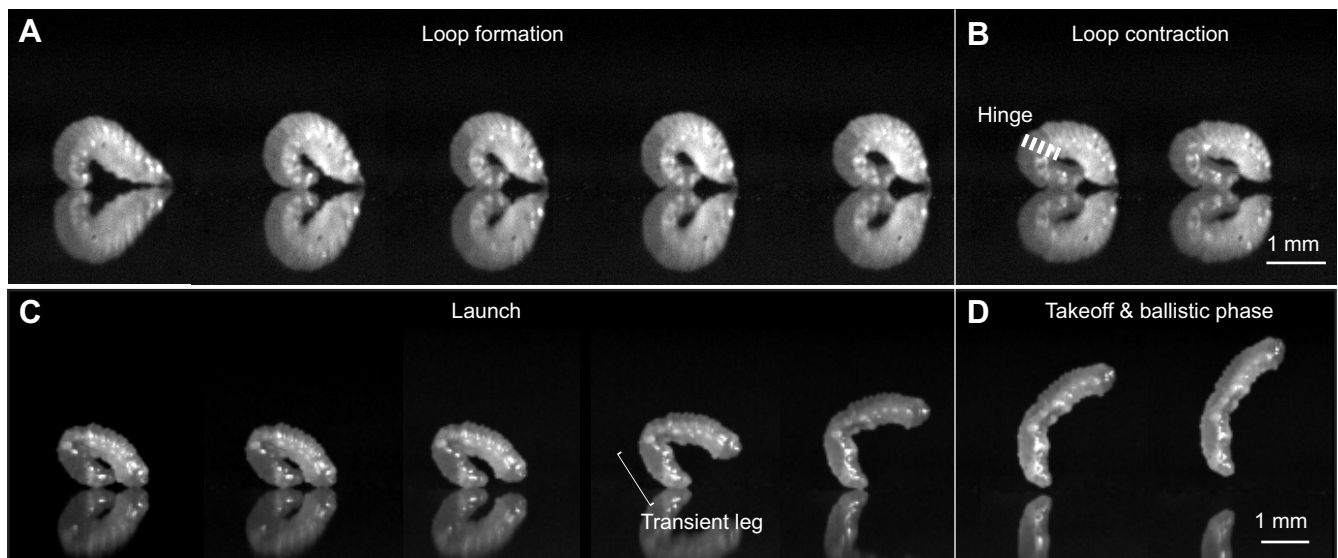
Fig. 3. Larvae launch themselves into the air using a latch mechanism, hydrostatic pressurization of their bodies and the formation of a transient leg. (A) The first phase of jump preparation is loop formation. The larva plants one end of its body, slides the other end towards it, and forms a circular loop held together by a latch mechanism. (B) The second phase of jump preparation is loop contraction. The larva begins hydrostatically pressurizing its body, compressing the loop, and forming a kink or transient hinge (white dashed line) at the posterior third of its body. (C) The anterior portion of the body moves upward when the latch is released. The hinge delineates a transient leg (white bracket) from the rest of the body, which applies force against the substrate and launches the larva into the air. Note that this time period – the moment of latch release until takeoff from the substrate – constitutes the duration and distance measured for launch kinematics (Table 1). (D) The larva becomes airborne during the ballistic phase. Takeoff is defined as the moment the animal leaves the ground. Images from A and B are taken from one video (0.16 s between images); images from C and D are from another video sequence (0.035 s between images).

19%; power: 21%; mass-specific power: 21%) and is represented via the significant digits of the results for both takeoff and launch.

We measured horizontal jump travel distance from jump origin to landing location using a ruler (resolution: 1 mm) on the benchtop. Larvae bounced slightly upon landing, potentially changing measured jump distance by a few body lengths. We did not film these jumps, because their travel distance was too far to capture simultaneously with the takeoff kinematics using extremely high-speed imaging.

Cost of transport, in terms of energy per distance per mass, was estimated for gall midge jumps. We combined average horizontal jump distance from the benchtop ruler measurements with the average takeoff angle measured from high-speed imaging (Table 1), and validated that takeoff speeds measured from the high-speed imaging were congruent with takeoff speeds predicted from the standard ballistics equation $d=2v^2\sin(\theta)\cos(\theta)g^{-1}$, where θ is the elevation angle of the jump and g is the acceleration due to gravity (Meriam and Kraige, 2010). We did not incorporate drag or spin losses. We then calculated the kinetic energy required to generate this takeoff velocity, divided that by the average jump distance, again yielding a conservative estimate of energy per unit distance (J m^{-1}). Lastly, we divided the calculated energy per unit distance (J m^{-1}) by the average larval mass (Table 1) to yield an estimate of the energy density required (J m^{-1} kg^{-1}) to traverse a given distance.

We performed linear mixed models (*lme4*) in R to assess the associations among body size and kinematics (v.1.1.442, RStudio, Boston, MA, USA; http://www.R-project.org/; Bates et al., 2015). R code, including the statistical models, is available in the associated archival data (Dryad deposition, dryad.jc5745v). Using linear mixed modeling, we compared models to identify how launch distance, launch duration and body mass influence takeoff speed. All models included takeoff speed as the dependent variable and

individual ID as the random effect. The null model was a reduced model including takeoff speed as the dependent variable. The other models used different independent variables: launch duration, launch speed, interaction of launch distance and launch duration, and interaction of launch distance and body mass.

We compared a second set of linear mixed models to assess the effect of body size and launch duration on launch distance, specifically through comparison of a reduced model as the null model, a second model with launch duration as the independent variable, and a third model with the interaction of body size and launch duration as the independent variable.

The sample sizes for all of the statistical models were 31 observations across 10 groups (individual ID) (Table 1). We modeled slopes and intercepts as random for all linear mixed models. Before comparing model fits, we tested each model's residuals for normality (shapiro.test) and if the residuals were not normal, then that model was not included in the final model comparison. The model that best fitted the data was determined through relative ranking based on the Akaike information criterion (AIC; lower AIC score indicates better model fit).

Latch morphology
We used scanning electron microscopy (SEM) to view the external morphology of the two body surfaces that form the latch. The larvae were difficult to preserve effectively for SEM, so we tried two different methods and report both here so that future investigators can benefit from these efforts. One group of larvae was placed in a 2.5% glutaraldehyde and 0.1 mol l^{-1} saline buffer solution and then transferred stepwise to a 100% ethanol solution. Specimens were then dried using a critical point dryer (CPD3, Ladd Research Industries, Williston, VT, USA), gold sputter coated (Desk IV, Denton Vacuum, Moorestown, NJ, USA), and imaged using a scanning electron

Table 1. Jump kinematics based on high-speed imaging and body size

No. of jumps	Body length (×10^{-3} m)	Body diameter (×10^{-3} m)	Body mass (×10^{-6} kg)	Launch distance (×10^{-4} m)	Launch duration (×10^{-3} s)	Average mass-specific power of launch (W kg^{-1})	Takeoff speed (m s^{-1})	Kinetic energy at takeoff (×10^{-7} J)	Takeoff angle (deg)
4	3.30	0.68	1.30	5.87 (3.72–7.70)	1.08 (0.85–1.25)	1150 (240–1750)	1.01 (0.56–1.26)	7.0 (2.1–10.2)	62 (58–65)
7	3.54	0.68	1.41	6.66 (2.46–9.29)	1.13 (0.80–1.60)	1260 (150–2160)	0.92 (0.47–1.18)	6.4 (1.5–9.7)	62 (54–64)
1	3.36	0.76	1.28	5.40	1.35	400	0.64	2.7	63
3	3.10	0.68	1.27	5.05 (3.91–6.00)	1.23 (1.15–1.35)	500 (210–700)	0.58 (0.39–0.72)	2.2 (1.0–3.3)	56 (55–58)
1	3.24	0.64	1.24	5.52	1.40	370	0.64	2.6	61
6	3.54	0.68	1.78	9.86 (7.37–12.15)	1.24 (1.05–1.45)	1750 (1170–2420)	1.18 (1.06–1.27)	12.4 (10.1–14.4)	67 (63–70)
2	3.60	0.72	1.45	7.25 (6.81–7.70)	1.52 (1.50–1.55)	500 (410–590)	0.87 (0.83–0.91)	5.5 (5.1–6.0)	66 (62–70)
1	2.44	0.50	0.50	2.88	0.70	810	0.70	1.2	63
3 (2)	3.46	0.66	1.24	7.03 (5.97–7.77)	1.17 (1.10–1.25)	1070 (780–1510)	0.91 (0.82–1.00)	5.2 (4.2–6.2)	68 (61–75)
3	3.28	0.68	1.26	6.35 (4.93–8.59)	1.00 (0.85–1.15)	1320 (1020–1620)	1.06 (0.97–1.11)	7.1 (5.9–7.8)	62 (61–66)
	3.28±0.33 (2.44–3.60)	0.68±0.06 (0.50–0.76)	1.27±0.32 (0.50–1.78)	6.19±1.79 (2.46–12.15)	1.18±0.23 (0.70–1.60)	910±470 (150–2420)	0.85±0.20 (0.39–1.27)	5.2±3.3 (1.0–14.4)	63±3 (54–75)

Data are mean and range (as appropriate); each row represents data from an individual gall midge, and the final row includes the mean, s.d. and range for each column. For the number of jumps, the count in parentheses refers to the takeoff data in the one case for which the launch dataset was larger than the takeoff angle dataset because of a short-duration video sequence.
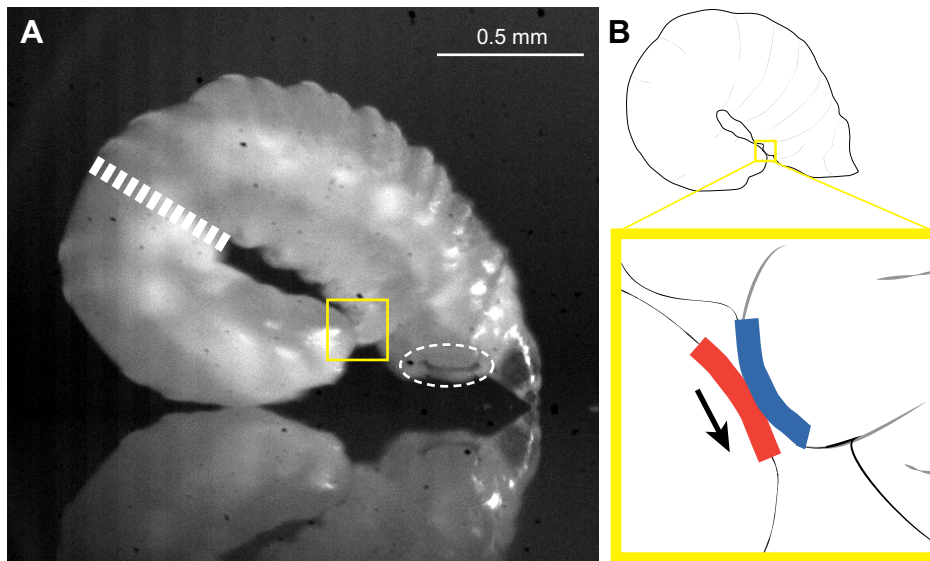
Fig. 4. A latch is formed by the opposing ventral surfaces of the third segment and posterior-most segment. (A,B) The latch (yellow box) consists of a ventral protrusion on the third segment that interacts with the posterior-most end of the larva's body. (A) Once the two surfaces latch together during loop formation (Fig. 3A), loop contraction occurs (Fig. 3B) and a transient hinge or kink (white dashed line) develops at the posterior third of the body. The posterior third of the larva becomes swollen and smooth, while the normal body ridges remain visible along the anterior portion of the body. The sternal spatula (white dashed ellipse) is visible and does not contribute to the latch mechanism. The anterior end of the body is furthest to the right. (B) Micro-scale, finger-like microstructures (see Fig. 8) on the third segment (blue line) and the posterior-most segment (red line) touch during latching. The latch releases and the posterior segment moves downward (arrow) and pushes against the substrate.

microscope (XL30 FEG-SEM, FEI, Hillsboro, OR, USA) (n=2 larvae). The second group was placed in boiling water and preserved in 70% ethanol. Specimens were dehydrated stepwise through hexamethyldisilazane (HMDS) and 100% ethanol solutions (15 min each in this order: 1:2 HMDS:ethanol; 1:1 HMDS:ethanol; 2:1 HMDS:ethanol; 100% HMDS). The specimens were placed in a fume hood and the fluid was evaporated for 1–24 h. Specimens were then mounted on stubs and imaged using SEM (n=2 larvae).

The boiling water/70% ethanol/HMDS preservation method yielded superior SEM images compared with the glutaraldehyde/100% ethanol/CPD preservation. Glutaraldehyde evidently failed to fully penetrate the larvae, such that the interior decayed, turning the larvae black/brown in color. This, or perhaps the stepwise transfer into 100% ethanol, also caused shriveling, such that the SEMs were not reliable. Therefore, all images and results reported here are based on the boiling water method.

The SEMs revealed that the latching areas of the body are covered with microstructures. We measured the dimensions of the microstructures and the area of the regions covered by these structures in order to assess the role of adhesion and friction in this latch mechanism. Microstructure width was measured from SEM images in ImageJ (ImageJ v.1.51n). To obtain an average size of the microstructures, 10 microstructures were measured on both the third body segment and the posterior-most end of the larva's body. The areas of these two microstructure regions were measured by tracing the area using the polygon selection tool in ImageJ. Because measurements of a three-dimensional surface were taken using a two-dimensional image, measurements are approximate.

Larvae were tested for the presence of resilin (GFPSirius M205FA/M165FC filters, excitation nm AT350/50x, emission nm ET420/50m, band-pass; L6000, Leica Microsystems Inc., Buffalo Grove, IL, USA) (n=3 larvae). Resilin is an elastomeric protein in arthropods that autofluoresces under ultraviolet light (Anderson, 1963, 1966).

RESULTS

### Jump preparation, launch dynamics and horizontal travel distance

Following previous terminology (Campbell and Kaya, 1999a,b; Maitland, 1992), jump preparation occurred in two phases: loop formation and loop contraction (Fig. 3A,B; Movie 1). Loop

formation began when one end of the body was positioned on the substrate. Then, the other end slid along the ground until the tip of the posterior end connected with the ventral side of the head segment (Fig. 4, yellow square), thereby forming a latch. Once latched, the body formed a circular shape, balancing on the dorsal side of the tail and the tip of the head (Fig. 3A). Loop formation averaged 1.79±0.34 s (n=2 larvae, 3 jumps, 1–2 jumps per larva).

Loop contraction (Fig. 3B) began when the body started to compress, distorting the circular shape. During this phase, a hinge or kink (Fig. 3B, white dashed line) appeared between the middle third and posterior third of the body, forming what we term a 'transient leg' (Fig. 3C, white bracket). Simultaneously, the 'leg' swelled, evidenced by smoothing of the body's ridges and folds, even as the ridges and folds were still visible on the anterior and middle thirds of the body. Loop contraction averaged 1.60±0.81 s (n=6 larvae, 9 jumps, 1–2 jumps per larva). Loop contraction ended when the latch
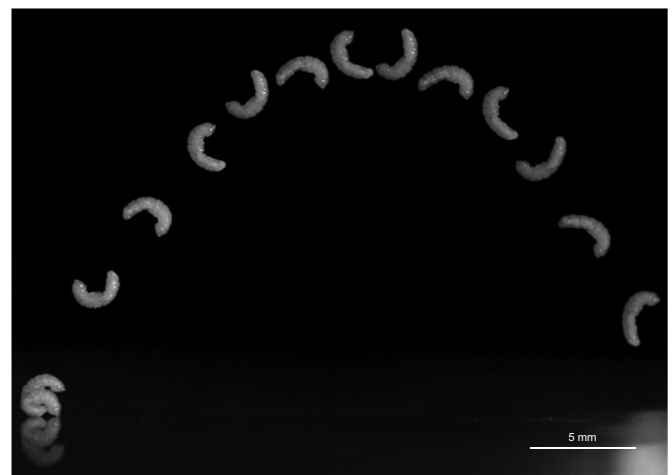
Fig. 5. Once the larvae are airborne, they follow a ballistic trajectory. Overlaid high-speed images of a larva's ballistic trajectory (0.0078 s between images, total duration of 0.11 s). Jumping larvae typically retain a slight bend at the transient hinge (Figs 3B and 4) and they rotate around their center of mass. The jump depicted in this figure is uncharacteristically short and was chosen so that the whole jump could be visualized in this figure using high-speed images. The jump distance dataset analyzed in this study (Table 2; average jump distance 77 mm) was not collected using high-speed imaging.
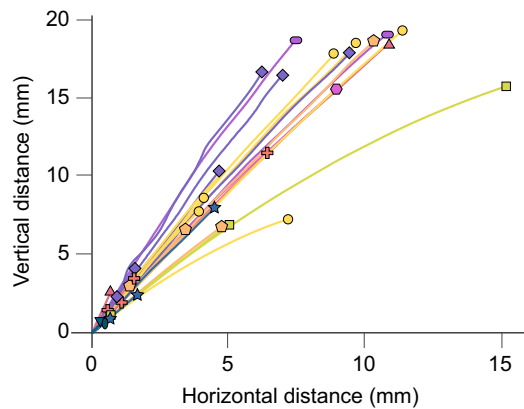
Fig. 6. Initial jump trajectories vary slightly within and between individuals. Each colored line and symbol represents a tracked initial jump trajectory of an individual larva (n=9 larvae, 30 jumps, 1–7 jumps per larva). One larva was not included in this plot, but does appear in Fig. 7, because its trajectory was so long that it reduced the ability to view the other jump trajectories.

was released, simultaneously pushing the transient 'leg' against the surface of the substrate and propelling the anterior end of the larva upward (Fig. 3C; Movie 2). The larvae spun as they followed a ballistic trajectory through the air, retaining a slight bend at the hinge, with the example in Fig. 5 spinning at 40 Hz (Fig. 3D, Fig. 5; Movie 3). Fig. 6 shows the trajectory of each jump until the larva was out of focus or left the field of view.

Power density during launch was on average 910 W kg^{-1} and reached a maximum of 2420 W kg^{-1} (Table 1). Launch distance was marginally better explained by the interaction between launch duration and body mass [log likelihood estimate (LL)=230, AIC=−444], when compared with the model with only launch duration (Fig. 7A) (LL=223, AIC=−433) and the null model (LL=221, AIC=−431). The residuals of the takeoff speed model containing the interaction between launch distance and duration were non-normally distributed; therefore, we did not include that model in the final model comparison. Among the remaining models, takeoff speed was best explained by launch distance (Fig. 7B) (LL=15, AIC=−17), followed by the interaction of launch distance and body mass (LL=14, AIC=−13). The remaining models had AIC scores above 0.

Larvae jumped as far as 121 mm (36.2 times their body length), with an average of 77.2±12.2 mm (range: 49–121 mm), which is

equivalent to 23.1±3.6 times their body length (n=5 larvae, 26 jumps, 2–11 jumps per larva). Average takeoff speed calculated using the ballistics equation and these jump distances was 0.97 m s^{-1}, and is similar to the average takeoff speed measured from high-speed imaging (0.85 m s^{-1}) (Table 1). Using average jump distance, takeoff angle and body mass (Table 1), we calculated that an average of 6.6 J kg^{-1} m^{-1} transport cost is required for gall midge jumps.

Latch morphology
The larvae were delicate and did not respond well to preservation techniques. The boiling water/70% ethanol/HMDS method yielded superior results, but still had drawbacks. Boiling water may have killed bacteria inside the gut (Martin, 1978), thus preventing the decay found in glutaraldehyde-preserved larvae. About 20% of larvae preserved with this method were in excellent condition for SEM, with minor cracking (which could be due to handling while mounting larvae on SEM stubs) and little to no shriveling. However, 80% of larvae preserved with this method were shriveled, deflated and generally in an unusable condition. It is unclear why the success rate was so low and what caused the differences in preservation outcome.

Even with these technical challenges, we were able to visualize the latch surfaces in multiple specimens. The latch is formed between the posterior-most region of the body and the ventral side of the third body segment. Bands of micrometer-scale, finger-like projections spanned the ventral body surface at each body segment, including the third body segment where the latch is located. The projections were oriented posteriorly in the SEM (Fig. 8). These microstructures were an average of 1.12±0.03 µm wide on the third body segment (Fig. 8, top row), and 1.14±0.08 µm on the posterior-most end of the body. The total area of the field of microstructures was 2.73×10^4 µm^2 on the third segment and 1.69×10^4 µm^2 on the posterior-most segment. The tip of the tail exhibited two large, semi-spherical pads dorsal to the finger-like microstructures (Fig. 8, bottom row). Autofluorescence was not observed during the test for resilin.

DISCUSSION
Larvae of *Asphondylia* sp. are small, worm-like jumpers that use hydrostatic body deformation and associated behaviors that are similar to those of previously described larval insect jumpers. Our study revealed the presence of an intriguing adhesive latching mechanism that mediates elastic energy storage and releases
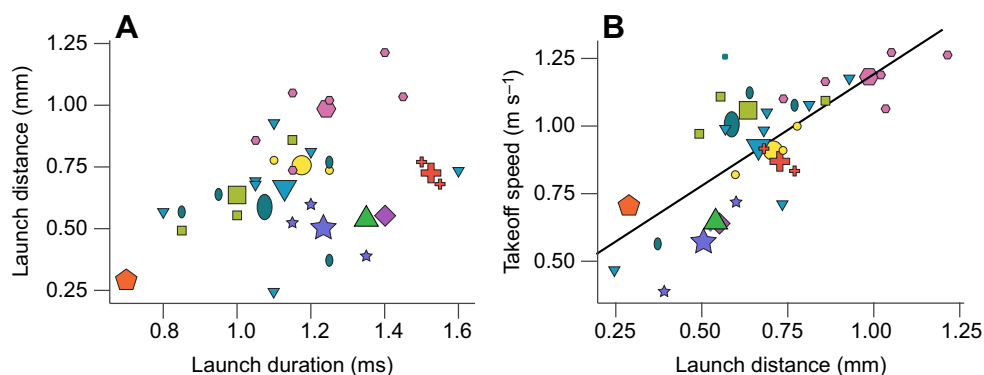
Fig. 7. Associations among launch parameters and takeoff speed. (A) Launch duration weakly predicts launch distance. (B) Takeoff speed is best predicted by the interaction between launch distance and individual. Each colored symbol represents an individual larva. Small points represent a single jump; large points represent the mean of all jumps performed by each individual. Sample sizes in both images are n=10 larvae, 31 jumps, 1–7 jumps per larva. The linear fit in B is based on the best-fit linear mixed model results for the two parameters, using the slope and coefficient of the fixed effect (see Results).
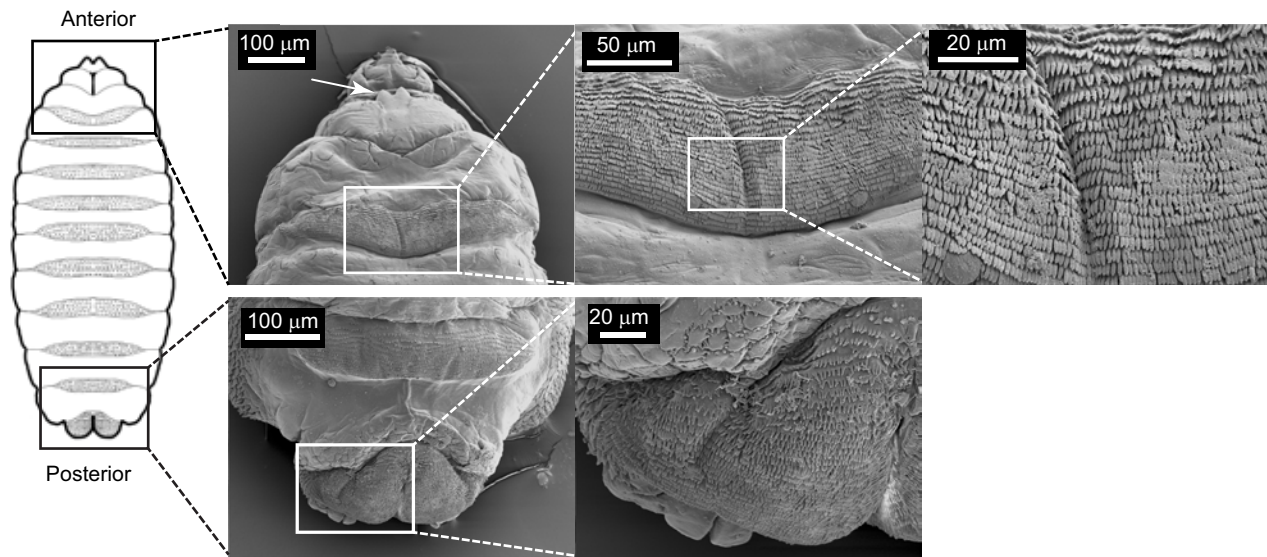
Fig. 8. Scanning electron micrographs (SEM) reveal micrometer-scale, finger-like microstructures that likely form a latch during jump preparation. Top row: images depict the ventral view of the anterior end of the larval body. Bands of finger-like microstructures span the width of each body segment, beginning with the third segment, and are oriented posteriorly. The sternal spatula (arrow) can be seen on the second segment. Bottom row: images are of the ventral view of the posterior end of the larval body. Finger-like microstructures are also oriented posteriorly. Measurements of the microstructure regions were taken from the two left-most images.

impressive launch kinematics and horizontal travel distances. Improved high-speed imaging capabilities yielded greater resolution of the energetics and dynamics of these jumps and place this class of locomotor system as being as effective as that of equivalently sized legged jumpers. Small, soft-bodied jumpers ultimately achieve an effective and energetically efficient locomotor system through a combination of hydrostatic manipulation, elastic energy storage and latching mechanics.

Kinematics, energetics and jump mechanics
The mass-specific power outputs of gall midge larval jumps are equivalent to or exceed the known capabilities of high-power vertebrate flight muscle (e.g. 400 W kg^{-1}; Askew and Marsh, 2002), and therefore support the hypothesis that they are not muscle powered and are instead driven by an elastic mechanism. The larvae generate impressive mass-specific power output during launch (Table 1; mean: 910 W kg^{-1}; maximum: 2420 W kg^{-1}). Comparison with the high-power muscle of vertebrate flyers may not be the appropriate threshold for testing for the presence of elastic energy in these larvae: extreme 'power-amplified' systems in arthropods, such as those found in trap-jaw ants and mantis shrimp, use force-modified, slowly contracting muscle to load stiff springs rather than high-power muscle (Ilton et al., 2018; Patek et al., 2006; Blanco and Patek, 2014; Gronenberg and Ehmer, 1996).

Therefore, given that they are unlikely to be using high-power muscles, gall midge larvae are almost certainly using elastic energy storage to power their jumps to achieve such high power densities. They appear to store elastic energy in their exoskeleton through manipulation of hydrostatic pressure and associated body deformation (Kier, 2012). We did not detect resilin during external tests of the cuticle. However, Maitland (1992) was able to experimentally store appreciable elastic strain energy in the body walls of another larval jumping insect species, suggesting that either resilin is present in deeper layers of the cuticle or that stiff, deformable cuticular or composite structures are used for elastic energy storage (e.g. Burrows et al., 2008).

In preparation for a jump, the larvae deform their body to form a transient leg, and then launch the body when this effective lever arm is pushed against the ground, similar to previously studied jumping of Mediterranean fruit fly larvae (Maitland, 1992). Once latched (Fig. 3B), the transient leg appears to swell, either through pressurized compartmentalized fluid in this region or by the use of a hydraulic mechanism that moves fluid into the posterior end of the body. This pressurization is visible as the smoothing of ridges and folds in the transient leg (Fig. 4A) during the loop contraction phase (Fig. 3B). A transient hinge, formed along the posterior third of the body, creates this transient leg that launches the jump. At first glance, this transient hinge appears to be a mechanical instability, like a 'kink', that ought to be avoided in cylindrical systems (Wainwright, 1988). However, given that this 'kink' remains visible throughout the jump (Fig. 5), it is possible that there are controlled internal structures that form this constriction and that the transient hinge is not an instability. Future studies would benefit from examining the timing of the contraction phase and its effect on the energetics of the jump.

Given that elastic energy storage and latch-mediated control enable larvae to travel horizontally from 20 to 30 times their body length, how do the energetic costs of locomoting via legless jumping compare with those of worm-like crawling (Walton et al., 1990)? Here we consider a back-of-the-envelope comparison of the energetic costs of these two modes of locomotion. Assuming no energy losses in the musculature, the energetic cost of moving via jumping in *Asphondylia* sp. larvae is approximately 8 J kg^{-1} m^{-1} (i.e. it takes 8 J of kinetic energy for the animal to move 1 kg of mass 1 m). Given that muscles are typically between 10% and 50% efficient in transferring metabolic energy to mechanical work depending on the species and the mechanics of muscle contraction (Smith et al., 2005), we can multiply larval jumping energy costs by 10 to account for the metabolic energy costs of the underlying muscle contraction, giving a jumping energy cost on the order of 80 J kg^{-1} m^{-1}. A previous analysis of the cost of transport of larval blowfly locomotion yielded crawling costs of the order of

$2300\ \text{J kg}^{-1}\ \text{m}^{-1}$ (Berrigan and Lighton, 1993). This difference, $80\ \text{J kg}^{-1}\ \text{m}^{-1}$ for larval, legless jumping compared with $2300\ \text{J kg}^{-1}\ \text{m}^{-1}$ for larval crawling, suggests one hypothesis for the advantages of small, worm-like jumping: jumping is far more energetically efficient than crawling an equivalent distance.

Latch mechanics

Based on high-speed imaging (Movie 2), we found that the latch does not involve mouthparts, as has been reported in piophilid or tephritid larvae (Bondurianksy, 2002; Marinov et al., 2015; Maitland, 1992). Additionally, microscopy showed no evidence of legs or protolegs that could be used to aid in latching, as hypothesized in larval fungus gnats (Camazine, 1986). Related species of gall midge outside the Asphondylinii tribe use a hard structure adjacent to the mouth, called the spatula, to exit the gall and burrow into the substrate just prior to the pupal stage (Gagné, 1994; Milne, 1961; Pitcher, 1957). Contrary to early conjectures on the function of the spatula found in third-instar larvae of most families of gall midges (Milne, 1961), the latch is not the sternal spatula (Figs 2 and 4, dashed white ellipse). The spatula is located anterior to the latching mechanism (Fig. 4, yellow square).

Instead, the latch in Asphondylia sp. larvae appears to operate via micro-scale, surface interactions. Hairy adhesive pads function by increasing surface area contact between the organism and the substrate by using micrometer- or nanometer-scale protrusions that can achieve close contact with even-textured surfaces (Federle, 2006; Clemente et al., 2017; Biewener and Patek, 2018). The finger-like microstructures seen on both the posterior-most section of the larva and the third segment are at the same scale as adhesive structures found in independently evolved arthropod larvae, adult insects and even gecko foot pads that use van der Waals interactions to facilitate attachment (Gao and Yao, 2004; Autumn et al., 2002). These microstructures are most likely acanthae, 'hairs' that originate from a single cell. This type of hair is common in Diptera, as opposed to the socketed setae more common in Coleoptera and Dermaptera (Arzt et al., 2003; Scherge and Gorb, 2001).

Adhesive mechanisms can attach organisms long term or temporarily to surfaces or other organisms, or create interactions between body parts (Gorb, 2002). The gall midge larval latch system may operate like the rarely observed interlocking fields of microstructures found in the dragonfly and damselfly head-arresting system (Gorb, 2002). The orientation of their microstructures is such that, when the larvae curl in preparation to jump, the microstructures could oppose and interlock with each other. Similar mechanisms have been found in wing-locking devices used to hold forewings and hindwings in place during flight, or to lock wings to the side of the insect's body during rest (Gorb, 2002; Gorb and Goodwyn, 2003). Another possibility is that the larvae excrete adhesive fluids that further enhance interaction between surfaces of the latch by filling in gaps between microstructures, a common adhesion mechanism in insects (Arzt et al., 2003).

The angle and orientation of these microstructures could also be important in determining attachment strength. Changes in gross body position can create a change in microstructure angle, by which the organisms can easily attach or detach (Federle, 2006). The larvae may release the latch mechanism (whether frictional or interlocking) by hydrostatically deforming the body, changing the angle or density of the microstructures, and thereby decreasing the interaction between the third segment and posterior segment surfaces. When the latching forces are overcome, stored energy in the cuticle is released, and the larva launches into the air. The dynamic control and release of latching forces is increasingly

recognized as a key part of the control of high-acceleration systems (Ilton et al., 2018).

Finger-like microstructures are found not just on the third body segment but across multiple body segments. The larvae may use them for adhesion to surfaces during locomotion, as has been implicated in other insect larvae (Hasenfuss, 1999). However, Hassenfus (1999) focused on larvae with protolegs (unlike Asphondylia sp. larvae). In addition, unlike the patches of finger-like protrusions in the Asphondylia sp. larvae, the adhesive structures were hooked and arranged in rings around the ends of protolegs. It may be that the outgrowths on Asphondylia sp. larvae aid in crawling locomotion. Uniformly sloped outgrowths allow for directional motion, as the angle of the outgrowths enables forward motion while simultaneously preventing backwards motion using peristaltic body movements (Gorb, 2002). The role of these finger-like microstructures in adhesion-based locomotion is intriguing, and may provide further insight into the locomotor abilities of soft-bodied, legless organisms.

The latch location of Asphondylia sp. larvae can be combined with their jump kinematics to estimate how much force the latch requires to hold everything in place. During a jump, the distal end of the transient leg (Fig. 3C, white bracket) generates an average ground reaction force of 0.60 mN ($470\ \text{m s}^{-2}$ multiplied by an average body mass of 1.27 mg; see Table 1). Just prior to the jump, the muscles must be able to build up that amount of force while the body is held by the latch. The latch is located at the distal tip of the transient leg, allowing for a simple estimate of latch adhesive forces using lever mechanics. While the body muscles contract, the latch must hold everything in place, resisting a maximum of 0.60 mN of force before it releases. The posterior-most groups of microprojections had an area of 16,900 μm^2 (Fig. 8, bottom row). To hold the body in place, the microstructures would have to generate $3.7\times10^4\ \text{N m}^{-2}$ of adhesion. Similar microstructures on the feet of leafhoppers (the tibial platellae) generate $1.25\times10^6\ \text{N m}^{-2}$ of adhesive force during a jump (Clemente et al., 2017), indicating that microstructures are able to generate more than enough force to be used as a latch in the gall midge larvae.

Diversity and kinematics of legless jumpers

Despite their lack of legs and rigid exoskeleton, the gall midge larvae jump with speeds comparable to those of fleas (Sutton and Burrows, 2011), and they achieve launch accelerations far exceeding those of another 'legless' jumper, the click beetle, which flexes its body to release energy stored in a hinge mechanism located between the body segments (Evans, 1972, 1973; Ribak and Weihs, 2011; Ribak et al., 2012).

Soft-bodied jumpers have been observed in two phyla and eight families: Steinernematidae (Campbell and Kaya, 1999a,b; Reed and Wallace, 1965), Tephritidae (Maitland, 1992; Suenaga et al., 1992), Mycetophilidae (Camazine, 1986), Piophilidae (Bondurianksy, 2002), Ichneumonidae (Day, 1970; Saeki et al., 2016), Thyrididae (Humphreys and Darling, 2013), Drosophilidae (Marinov et al., 2015) and Cecidomyiidae. There are over 6203 known species and 736 genera in the family Cecidomyiidae distributed throughout the world (Gagné and Jaschhof, 2014), several of which have been reported to jump (Tokuhisa et al., 1979; Manier and Deamer, 2014; Milne, 1961), suggesting an abundance of subjects for studying hydrostatic jumping mechanisms (Table 2). However, only a handful of studies have examined the jumping biomechanics of soft-bodied, legless jumpers (Campbell and Kaya, 1999a,b; Reed and Wallace, 1965; Bondurianksy, 2002; Maitland, 1992; Milne, 1961; Table 2). Our study thus offers the most inclusive dataset on

Table 2. Kinematic capabilities of soft-bodied legless jumpers

	Asphondylia sp. (gall midge larva)	Steinernema carpocapsae (nematode)	Mycetophila cingulum (fungus gnat larva)	Ceratitis capitate (Mediterranean fruit fly larva)	Prochyliza xanthostoma (carrion fly larva)	Neuroterus saltatorius (gall forming wasp larva)	Calindoea trifascialis (southeast Asian moth caterpillar)	Contarinia inouyei (cedar gall midge larva)
Frame rate (frames s⁻¹)	20,000	30	54	25	–	–	–	–
Body mass (×10⁻⁶ kg)	1.27±0.32 (0.50–1.78) (10, 1–7)	2.18×10^{-6} (–) (–)	–	17±1.9 (–) (20)	–	–	–	–
Body length (×10⁻³ m)	3.28±0.33 (2.44–3.60) (10, 1–7)	0.558 (–) (–)	8 (–) (–)	–	(4–7) (89)	–	–	–
Jump distance (×10⁻³ m)	76.7±18.6 (42–121) (5, 2–11)	0.48±0.08 (0.06–1.32) (33)	95±28 (–) (–)	120±0.8 (–) (16)	– (200–500) (–)	– (10–30) (–)	7.5 (–) (–)	62.8±21.0 (–) (21)
Speed (m s⁻¹)	0.88±0.21[T] (0.38–1.33) (10, 1–7)	1.13[U] (–) (–)	–[U] (0.81–1.50) (–)	0.5[U] (–) (–)	–	–	–	–
Acceleration (m s⁻²)	880±210[T] (380–1330) (10, 1–7)	1608.5[U] (–) (–)	2340[L] (–) (–)	835.7[U] (–) (–)	–	–	–	–
Energy per jump (J)	$5.6\times10^{-7}\pm3.4\times10^{-7}$[T] ($0.9\times10^{-7}$–$14.5\times10^{-7}$) (10, 1–7)	–	–	–	–	3.1×10^{-8}[T] (–) (–)	–	–
Citation	Present study	Campbell and Kaya, 1999a,b	Camazine, 1986	Maitland, 1992	Bonduriansky, 2002	Manier and Deamer, 2014	Humphreys and Darling, 2013	Tokuhisa et al., 1979

Soft-bodied legless jumpers have been reported in 8 families across 2 phyla. Data for each species (common name in parentheses) are presented as means (±s.d. where available); data in parentheses are the range, and the number of larvae, number of jumps per larvae. A dash indicates that data were not reported in the publication. [L]Measured launch period. [T]Measured or calculated takeoff period. [U]Unspecified or unresolved (because of low frame rates) time period for jump takeoff, launch, or both.

larval jumping kinematics, including launch speed, acceleration, power and energy. Most other studies report only a few of these metrics (Table 2). Additionally, by filming at an appropriately fast frame rate, we are able to report more accurate kinematics than previous studies. Even so, at these small scales and fast kinematics, even our calculations have error uncertainties of up to 20%, largely arising from the resolution limits of the scale bar.

Relatively little is known about the role of jumping in the life history of these larvae. Larvae of most cecidomyiid species exit their galls at the end of their third instar, fall to the ground, and use their sternal spatula to burrow into the soil, where they then pupate (Sen, 1939; Milne, 1961; Pitcher, 1957; Dorchin et al., 2015). Prior to burrowing, larvae jump in order to locate a suitable location for pupation. Jumping has been shown in a variety of taxa to help larvae avoid desiccation, escape predation and parasitization, and avoid lethal temperatures (Humphreys and Darling, 2013; Manier and Deamer, 2014; Maitland, 1992; Day, 1970; Saeki et al., 2016). The cecidomyiid groups that do not pupate in the soil develop through all three larval instars and pupate in the gall, emerging only as adults. These include Asphondyliina (the subtribe to which *Asphondylia* sp. belongs), as well as a smattering of other species throughout the family Cecidomyiidae (Gagné, 1994; Uechi and Yukawa, 2006). Current understanding of this group suggests that these larvae never jump, as they are confined in the gall during the only point in development when jumping behavior is exhibited. Therefore, it is possible that *Asphondylia* sp.'s jumping ability is an evolutionary relic that served a purpose in their ancestors (pupation in soil is the ancestral state for Cecidomyiidae: Tokuda and Yukawa, 2007; Gagné, 1994; Tokuda, 2012).

However, we have observed that *Asphondylia* sp. removed from their galls during the third larval instar are able to jump upon the substrate, burrow into soil, pupate and emerge as adults (M.J.W., personal observation). Additionally, their jumping behavior is robust, as evidenced by their impressive kinematics and ability to jump multiple times. In combination, these observations suggest that the sternal spatula, latch mechanism and jumping ability are not mere evolutionary remnants from when they diverged from a burrowing ancestor. It remains uncertain, however, under what conditions larvae would leave their galls, thereby necessitating pupation in the soil. Studies on other gall midges of goldenrods have shown that rosette galls like those induced by *Asphondylia* sp. are ecologically busy locations (Crawford et al., 2007). Gall chambers are invaded by insect predators, parasitoids, inquilines and chewing herbivores that feed on plant tissue that make up the galls (Dorchin et al., 2007, 2009, 2015). Thus, it is not uncommon for the inhabitants of galls to be disturbed as their chambers are breached. If released from their galls, the ability to jump to escape predators or to quickly find a suitable burrowing site for pupation would therefore be advantageous. To better understand the natural history of this gall midge species and the potential function of its jumping, further behavioral analysis and field observations would be of great value.

Conclusions

With dramatic growth in the fields of small, high-acceleration systems (e.g. Ilton et al., 2018), soft robotics (e.g. Cianchetti et al., 2018; Rich et al., 2018; Sitti, 2018; Trimmer, 2018) and biological adhesion (Autumn et al., 2002; Gorb, 2002, 2005; Gorb and Goodwyn, 2003; Federle, 2006; Labonte and Federle, 2015; Labonte et al., 2016), the realm of small, worm-like, legless jumpers offers notable insights at the interface of these fields. These small larvae combine elastic energy storage and adhesive latching to achieve impressive launch kinematics and horizontal travel

distances that rival those of legged jumpers. Not only is there potential for discovery in future studies of the natural history and performance of jumping in *Asphondylia* sp. but also these findings bridge previous research across an array of similar, independently evolved systems and point toward an untapped and rich diversity of mechanically interesting biological mechanisms in soft-bodied, legless jumpers.

Author contributions
Conceptualization: M.J.W., S.N.P.; Methodology: G.M.F., J.S.H., G.P.S., S.N.P.; Formal analysis: G.M.F., S.N.P.; Investigation: G.M.F., M.J.W., J.S.H., C.K., S.N.P.; Resources: M.J.W., S.N.P.; Data curation: G.M.F., S.N.P.; Writing - original draft: G.M.F., S.N.P.; Writing - review & editing: G.M.F., M.J.W., J.S.H., G.P.S., C.K., S.N.P.; Visualization: G.M.F.; Supervision: S.N.P.; Project administration: S.N.P.; Funding acquisition: S.N.P.

Data availability
Data are available from the Dryad digital repository (Farley et al., 2019): dryad.jc5745v

Supplementary information
Supplementary information available online at
http://jeb.biologists.org/lookup/doi/10.1242/jeb.201129.supplemental

References
Aerts, P. (1998). Vertical jumping in *Galago senegalensis*: the quest for an obligate mechanical power amplifier. *Philos. Trans. R. Soc. Lond. B Biol. Sci.* **353**, 1607-1620. doi:10.1098/rstb.1998.0313

Alexander, R. M. N. and Vernon, A. (1975). The mechanics of hopping by kangaroos (Macropodidae). *J. Zool.* **177**, 265-303. doi:10.1111/j.1469-7998.1975.tb05983.x

Anderson, S. O. (1963). Characterization of a new type of cross-linkage in resilin, a rubber-like protein. *Biochim. Biophys. Acta.* **69**, 249-262. doi:10.1016/0006-3002(63)91258-7

Anderson, S. O. (1966). Covalent cross-links in a structural protein, resilin. *Acta. Physiol. Scand. Suppl.* **66**, 1-81.

Arzt, E., Gorb, S. and Spolenak, R. (2003). From micro to nano contacts in biological attachment devices. *Proc. Natl. Acad. Sci. USA* **100**, 10603-10606. doi:10.1073/pnas.1534701100

Ashley-Ross, M. A., Perlman, B. M., Gibb, A. C. and Long, J. H., Jr. (2014). Jumping sans legs: does elastic energy storage by the vertebral column power terrestrial jumps in bony fishes? *Zoology* **117**, 7-18. doi:10.1016/j.zool.2013.10.005

Askew, G. N. and Marsh, R. L. (2002). Muscle designed for maximum short-term power output: quail flight muscle. *J. Exp. Biol.* **205**, 2153-2160.

Astley, H. C. and Roberts, T. J. (2014). The mechanics of elastic loading and recoil in anuran jumping. *J. Exp. Biol.* **217**, 4372-4378. doi:10.1242/jeb.110296

Autumn, K., Sitti, M., Liang, Y. A., Peattie, A. M., Hansen, W. R., Sponberg, S., Kenny, T. W., Fearing, R., Israelachvili, J. N. and Full, R. J. (2002). Evidence for van der Waals adhesion in gecko setae. *Proc. Natl. Acad. Sci. USA* **99**, 12252-12256. doi:10.1073/pnas.192252799

Bates, D., Mächler, M., Bolker, B. and Walker, S. (2015). Fitting linear mixed-effects models using lme4. *J. Stat. Softw.* **67**, 1-48. doi:10.18637/jss.v067.i01

Bennet-Clark, H. C. (1975). The energetics of the jump of the locust *Schistocerca gregaria*. *J. Exp. Biol.* **63**, 53-83.

Bennet-Clark, H. C. and Lucey, E. C. A. (1967). The jump of the flea: a study of the energetics and a model of the mechanism. *J. Exp. Biol.* **47**, 59-76.

Berrigan, D. and Lighton, J. R. B. (1993). Bioenergetic and kinematic consequences of limblessness in larval diptera. *J. Exp. Biol.* **179**, 245-259.

Biewener, A. A. and Patek, S. N. (2018). *Animal Locomotion*. Oxford: Oxford University Press.

Blanco, M. M. and Patek, S. N. (2014). Muscle trade-offs in a power-amplified prey capture system. *Evolution* **68**, 1399-1414. doi:10.1111/evo.12365

Bonduriansky, R. (2002). Leaping behaviour and responses to moisture and sound in larvae of piophilid carrion flies. *Can. Entomol.* **134**, 647-656. doi:10.4039/Ent134647-5

Brackenbury, J. and Hunt, H. (1993). Jumping in springtails: mechanism and dynamics. *J. Zool.* **229**, 217-236. doi:10.1111/j.1469-7998.1993.tb02632.x

Burrows, M. and Sutton, G. P. (2008). The effect of leg length on jumping performance of short- and long-legged leafhopper insects. *J. Exp. Biol.* **211**, 1317-1325. doi:10.1242/jeb.015354

Burrows, M., Shaw, S. R. and Sutton, G. P. (2008). Resilin and chitinous cuticle form a composite structure for energy storage in jumping by froghopper insects. *BMC Biol.* **6**, 41. doi:10.1186/1741-7007-6-41

Camazine, S. (1986). Leaping locomotion in *Mycetophila cingulum* (Diptera: Mycetophilidae): Prepupation dispersal mechanism. *Ann. Entomol. Soc. Am.* **79**, 140-145. doi:10.1093/aesa/79.1.140

Campbell, J. F. and Kaya, H. K. (1999a). How and why a parasitic nematode jumps. *Nature* **397**, 485-486. doi:10.1038/17254

Campbell, J. F. and Kaya, H. K. (1999b). Mechanism, kinematic performance, and fitness consequences of jumping behavior in entomopathogenic nematodes (*Steinernema* spp.). *Can. J. Zool.* **77**, 1947-1955. doi:10.1139/z99-178

Cianchetti, M., Laschi, C., Menciassi, A. and Dario, P. (2018). Biomedical applications of soft robotics. *Nat. Rev. Mater.* **3**, 143-153. doi:10.1038/s41578-018-0022-y

Clemente, C. J., Goetzke, H. H., Bullock, J. M. R., Sutton, G. P., Burrows, M. and Federle, W. (2017). Jumping without slipping: Leafhoppers (Hemiptera: Cicadellidae) possess special tarsal structures for jumping from smooth surfaces. *J. Roy. Soc.* **14**, doi:10.1098/rsif.2017.0022

Crawford, K. M., Crutsinger, G. M. and Sanders, N. J. (2007). Host-plant genotypic diversity mediates the distribution of an ecosystem engineer. *Ecology* **88**, 2114-2120. doi:10.1890/06-1441.1

Day, W. H. (1970). The survival value of its jumping cocoons to *Bathyplectes anurus*, a parasite of the alfalfa weevil. *J. Econ. Entomol.* **63**, 586-589. doi:10.1093/jee/63.2.586

Dorchin, N., Clarkin, C. E., Scott, E. R., Luongo, M. P. and Abrahamson, W. G. (2007). Taxonomy, life history, and population sex ratios of North American *Dasineura* (Diptera: Cecidomyiidae) on goldenrods (Asteraceae). *Ann. Entomol. Soc. Am.* **100**, 539-548. doi:10.1603/0013-8746(2007)100[539:TLHAPS]2.0.CO;2

Dorchin, N., Scott, E. R., Clarkin, C. E., Luongo, M. P., Jordan, S. and Abrahamson, W. G. (2009). Behavioural, ecological and genetic evidence confirm the occurrence of host-associated differentiation in goldenrod gall-midges. *J. Evol. Biol.* **22**, 729-739. doi:10.1111/j.1420-9101.2009.01696.x

Dorchin, N., Joy, J. B., Hilke, L. K., Wise, M. and Abrahamson, W. G. (2015). Taxonomy and phylogeny of the *Asphondylia* species (Diptera: Cecidomyiidae) of North American goldenrods: Challenging morphology, complex host associations, and cryptic speciation. *Zool. J. Linnean. Soc.* **174**, 265-304. doi:10.1111/zoj.12234

Evans, M. E. G. (1972). The jump of the click beetle (Coleoptera, Elateridae) – a preliminary study. *J. Zool.* **167**, 319-336. doi:10.1111/j.1469-7998.1972.tb03115.x

Evans, M. E. G. (1973). The jump of the click beetle (Coleoptera: Elateridae) - energetics and mechanics. *J. Zool.* **169**, 181-194. doi:10.1111/j.1469-7998.1973.tb04553.x

Farley, G. M., Wise, M. J., Harrison, J. S., Sutton, G. P., Kuo, C. and Patek, S. N. (2019). Data from: Adhesive latching and legless leaping in small, worm-like insect larvae. *Dryad Digital Repository.* https://doi.org/10.5061/dryad.jc5745v

Federle, W. (2006). Why are so many adhesive pads hairy?. *J. Exp. Biol.* **209**, 2611-2621. doi:10.1242/jeb.02323

Gagné, R. J. (1994). *The Gall Midges of the Neotropical Region*. New York: Cornell University Press.

Gagné, R. J. and Jaschhof, M. (2014). *A Catalog of the Cecidomyiidae (Diptera) of the World.* 3rd edn. Digital version 2. Washington, DC, USA: U.S. Department of Agriculture.

Gao, H. and Yao, H. (2004). Shape insensitive optimal adhesion of nanoscale fibrillar structures. *Proc. Natl. Acad. Sci. USA* **101**, 7851-7856. doi:10.1073/pnas.0400757101

Gorb, S. N. (2002). *Attachment Devices of Insect Cuticle*. New York: Kluwer Academic Publishers.

Gorb, S. N. (2005). Uncovering insect stickiness: structure and properties of hairy attachment devices. *Am. Entomol.* **51**, 31-35. doi:10.1093/ae/51.1.31

Gorb, S. N. and Goodwyn, P. J. P. (2003). Wing-locking mechanisms in aquatic heteroptera. *J. Morphol.* **257**, 127-146. doi:10.1002/jmor.10070

Gronenberg, W. (1996). Fast actions in small animals: springs and click mechanisms. *J. Comp. Physiol. A* **178**, 727-734. doi:10.1007/BF00225821

Gronenberg, W. and Ehmer, B. (1996). The mandible mechanism of the ant genus *Anochetus* (Hymenoptera, Formicidae) and the possible evolution of trap-jaws. *Zool.* **99**, 153-162.

Hasenfuss, I. (1999). The adhesive devices in larvae of Lepidoptera (Insecta, Pterygota). *Zoomorph.* **119**, 143-162. doi:10.1007/s004350050088

Henry, H. T., Ellerby, D. J. and Marsh, R. L. (2005). Performance of guinea fowl *Numida meleagris* during jumping requires storage and release of elastic energy. *J. Exp. Biol.* **208**, 3293-3302. doi:10.1242/jeb.01764

Humphreys, K. and Darling, D. C. (2013). Not looking where you are leaping: a novel method of oriented travel in the caterpillar *Calindoea trifascialis* (Moore) (Lepidoptera: Thyrididae). *Biol. Lett.* **9**, 1-5. doi:10.1098/rsbl.2013.0397

Ilton, M., Bhamla, M. S., Ma, X., Cox, S. M., Fitchett, L. L., Kim, Y., Koh, J. S., Krishnamurthy, D., Kuo, C. Y., Temel, F. Z. et al. (2018). The principles of cascading power limits in small, fast biological and engineered systems. *Science* **360**, eaao1082. doi:10.1126/science.aao1082

Kier, W. M. (2012). The diversity of hydrostatic skeletons. *J. Exp. Biol.* **215**, 1247-1257. doi:10.1242/jeb.056549

Labonte, D. and Federle, W. (2015). Scaling and biomechanics of surface attachment in climbing animals. *Philos. Trans. R. Soc. B* **370**, doi:10.1098/rstb.2014.0027

Labonte, D., Clemente, C. J., Dittrich, A., Kuo, C. Y., Crosby, A. J., Irschick, D. J. and Federle, W. (2016). Extreme positive allometry of animal adhesive pads and the size of limits of adhesion-based climbing. *Proc. Natl. Acad. Sci. USA* **113**, 1297-1302. doi:10.1073/pnas.1519459113

Longo, S. J., Cox, S. M., Azizi, E., Ilton, M., Olberding, J. P., St. Pierre, R. and Patek, S. N. (2019). Beyond power amplification: latch-mediated spring actuation is an emerging framework for the study of diverse elastic systems. *J. Exp. Biol.* **222**. doi:10.1242/jeb.197889

Maitland, D. P. (1992). Locomotion by jumping in the Mediterranean fruit-fly larva *Ceratitis capitata*. *Nature* **355**, 159-161. doi:10.1038/355159a0

Manier, S. and Deamer, D. (2014). Jumping galls: a novel mechanism for motility. *J. Insect Biol.* **27**, 716-721. doi:10.1007/s10905-014-9462-4

Marinov, M., Li, D. and Bennett, S. (2015). An observation of leaping behaviour in larvae of Drosophilidae (Diptera). *The Weta* **50**, 30-37.

Martin, J. E. H. (1978). *The Insects and Arachnids of Canada, Part 1: Collecting, Preparing, and Preserving Insects, Mites, and Spiders*. Quebec: Kromar Printing Ltd.

Meriam, J. L. and Kraige, L. G. (2010). *Engineering Mechanics: Dynamics*, Eighth edition. Wiley and Sons. ISBN 978-1-118-88584-0.

Milne, D. (1961). The function of the sternal spatula in gall midges. *Physiol. Entomol.* **36**, 126-131. doi:10.1111/j.1365-3032.1961.tb00279.x

Moore, T. Y., Rivera, A. M. and Biewener, A. A. (2017). Vertical leaping mechanics of the Lesser Egyptian Jerboa reveal specialization for maneuverability rather than elastic energy storage. *Front. Zool.* **14**, 1-12. doi:10.1186/s12983-017-0215-z

Patek, S. N. (2015). The most powerful movements in biology. *Am. Sci.* **103**, 330-337. doi:10.1511/2015.116.330

Patek, S. N., Baio, J. E., Fisher, B. L. and Suarez, A. V. (2006). Multifunctionality and mechanical origins: ballistic jaw propulsion in trap-jaw ants. *Proc. Nat. Acad. Sci.* **103**, 12787-12792. doi:10.1073/pnas.0604290103

Patek, S. N., Dudek, D. M. and Rosario, M. V. (2011). From bouncy legs to poisoned arrows: elastic movements in invertebrates. *J. Exp. Biol.* **214**, 1973-1980. doi:10.1242/jeb.038596

Pitcher, R. S. (1957). The abrasion of the sternal spatula of the larva of *Daxyneura tetensi* (Rübs) (Diptera: Cecidomyidae) during the post-feeding phase. *Proc. R. Entomol. Soc. Lond. A Gen. Entomol.* **32**, 83-89. doi:10.1111/j.1365-3032.1957.tb00377.x

Reed, E. M. and Wallace, H. R. (1965). Leaping locomotion by an insect-parasitic nematode. *Nature.* **206**, 210-211. doi:10.1038/206210a0

Ribak, G. and Weihs, D. (2011). Jumping without using legs: the jump of the click-beetles (Elateridae) is morphologically constrained. *PLoS ONE* **6**, e20871. doi:10.1371/journal.pone.0020871

Ribak, G. Reingold. S. and Weihs, D. (2012). The effect of natural substrates on jump height in click-beetles. *Funct. Ecol.* **26**, 493-499. doi:10.1111/j.1365-2435.2011.01943.x

Rich, S. I., Wood, R. J. and Majidi, C. (2018). Untethered soft robotics. *Nat. Electron.* **1**, 102-112. doi:10.1038/s41928-018-0024-1

Saeki, Y., Tani, S., Fukuda, K., Iwase, S.-I., Sugawara, Y., Tuda, M. and Takagi, M. (2016). Costs and benefits of larval jumping behaviour of *Bathyplectes anurus*. *Sci. Nat.* **103**, 1. doi:10.1007/s00114-015-1324-1

Sakes, A., van der Wiel, M., Henselmans, P. W. J., van Leeuwen, J. L., Dodou, D. and Breedveld, P. (2016). Shooting mechanisms in nature: a systematic review. *PLoS ONE* **11**, e0158277. doi:10.1371/journal.pone.0158277

Scherge, M. and Gorb, S. (2001). *Biological Micro- and Nano-tribology: Nature's Solutions* (ed. P. Avouris, K. von Klitzing and R. Wiesendanger). New York: Springer.

Sen, P. (1939). On the function and development of the sternal spatula in the Cecidomyiidae or gall midges as exemplified by *Rhabdophaga saliciperda* Duf. *J. Morphol.* **65**, 1-15. doi:10.1002/jmor.1050650102

Sitti, M. (2018). Miniature soft robots - road to the clinic. *Nat. Rev. Mater.* **3**, 74-75. doi:10.1038/s41578-018-0001-3

Smith, N. P., Barclay, C. J. and Loiselle, D. S. (2005). The efficiency of muscle contraction. *Prog. Biophys. Molec. Biol.* **88**, 1-58. doi:10.1016/j.pbiomolbio.2003.11.014

Suenaga, H., Kamiwada, H., Tanaka, A. and Chishaki, N. (1992). Difference in the timing of larval jumping behavior of mass-reared and newly-colonized strains of

the melon fly, *Dacus cucurbitae* Coquillett (Diptera: Tephritidae). *Appl. Entomol. Zool.* **27**, 177-183. doi:10.1303/aez.27.177

Sutton, G. P. and Burrows, M. (2011). Biomechanics of jumping in the flea. *J. Exp. Biol.* **214**, 836-847. doi:10.1242/jeb.052399

Tokuda, M. (2012). Biology of Asphondyliini (Diptera: Cecidomyiidae). *Entomol. Sci.* **15**, 361-383. doi:10.1111/j.1479-8298.2012.00539.x

Tokuda, M. and Yukawa, J. (2007). Biogeography and evolution of gall midges (Diptera: Cecidomyiidae) inhabiting broad-leaved evergreen forests in oriental and eastern Palearctic regions. *Orient. Insects* **41**, 121-139. doi:10.1080/00305316.2007.10417502

Tokuhisa, E., Nagai, S. and Yukawa, J. (1979). Jumping behaviour of the larvae of the Japanese cedar gall midge, *Contarinia inouyei* Mani (Diptera: Cecidomyiidae). *Kontyû* **47**, 599-605.

Trimmer, B. A. (2018). Soft-bodied terrestrial invertebrates. In *Living Machines: A Handbook of Research in Biomimetic and Biohybrid Systems* (ed. T. Prescott, P. Vershure and N. Lepora), Oxford University Press.

Uechi, N. and Yukawa, J. (2006). Life history patterns and host ranges of the genus *Asphondylia* (Diptera: Cecidomyiidae). In *Galling Arthropods and Their Associates: Ecology and Evolution* (ed. K. Ozaki, J. Yukawa, T. Ohgushi and P. W. Price), pp. 275-285. Tokyo: Springer-Verlag.

Wainwright, S. A. (1988). *Axis and Circumference: The Cylindrical Shape of Plants and Animals*. Cambridge, MA: Harvard University Press.

Walton, M., Jayne, B. C. and Bennett, A. F. (1990). The energetic cost of limbless locomotion. *Science* **249**, 524-527. doi:10.1126/science.249.4968.524

Zajac, F. E., Zomlefer, M. R. and Levine, W. S. (1981). Hindlimb muscular activity, kinetics and kinematics of cats jumping to their maximum achievable heights. *J. Exp. Biol.* **91**, 73-86.